RELATIVISTIC DESCRIPTION OF BARYON PROPERTIES

Vladimir Galkin

Institute of Informatics in Education, FRC CSC RAS, Moscow

(in collaboration with Dietmar Ebert and Rudolf Faustov)

18-30 July 2016, BLTP, JINR, Dubna, Russia

INTRODUCTION

Convincing evidence of the existence of diquark correlations in hadrons has been collected

• In heavy meson sector several charged charmonium- and bottomonium-like states were discovered. They should be inevitably multiquark, at least four quark — tetraquark, states. One of the most successful pictures of such tetraquark states is the diquark-antidiquark model

• In light meson sector it has been argued for a long time that mesons forming inverted lightest scalar nonet can be well described as tetraquarks treated as diquark-antidiquark bound states

• In baryon sector the number of observed excited states both in light and heavy sectors is considerably lower than the number of excited states predicted in three-quark picture

– Introduction of diquarks significantly reduces the number of baryon states since some of degrees of freedom are frozen and thus the number of possible excitations is substantially smaller

Baryons:

- Triply heavy baryons QQQ $(Q = c, b)$

— no experimental data $\Longrightarrow$ will not be discussed

- Doubly heavy baryons qQQ $(q = u, d, s,\ Q = c, b)$ [PRD 66, 014008 (2002)]

— two heavy quarks form a diquark $d = QQ$

— excitations both in diquark and in quark-diquark systems are considered

— no reliable experimental data $\Longrightarrow$ will not be discussed

- Heavy baryons qqQ $(Q = c, b)$

— two light quarks form a diquark $d = qq$

— all excitations occur in the quark-diquark bound system (no internal diquark excitations)

— in the last few years the number of the observed charmed and bottom baryons almost doubled. Now it is nearly the same as the number of known charmed and bottom mesons.

— due to the poor statistics, the quantum numbers of most of the excited states of heavy baryons are not known experimentally and are usually prescribed following the quark model predictions

- Strange baryons sqq

— diquark is composed from quarks of the same constituent mass

— excitations occur both in the quark-diquark bound system and inside diquark

— ground and first orbital and radial excited states of light diquarks should be considered

— vast experimental data is available

— quantum numbers of most observed states are known

- N and Δ resonances qqq

— ground state nuclon (N) and Δ are well reproduced

— excitations have not been considered in our model yet $\Longrightarrow$ will not be discussed

Baryon spectroscopy

- Main assumption: quark–diquark picture of baryons

Three-body calculation $\longrightarrow$ two-step two-body calculation

- Diquark is a composite (qq') system:

– light diquark is not point-like object: Its interaction with gluons is smeared by the form factor expressed through the overlap integral of diquark wave functions

- Pauli principle for ground state diquarks:

– (qq') diquark can have $S = 0, 1$ (scalar $[q, q']$, axial vector $\{q, q'\}$)
– (qq) diquarks can have only $S = 1$ (axial vector $\{q, q\}$)

- Light quarks, light diquarks and heavy quarks are considered fully relativistically without v/c expansion

RELATIVISTIC QUARK MODEL

Relativistic quasipotential equation of Schrödinger type:

$$\left(\frac{b^2(M)}{2\mu_R} - \frac{\mathbf{p}^2}{2\mu_R}\right)\Psi_M(\mathbf{p}) = \int \frac{d^3q}{(2\pi)^3} V(\mathbf{p},\mathbf{q};M)\Psi_M(\mathbf{q})$$

$\mathbf{p}$ - center-of-mass relative momentum of quarks (diquarks)
M - bound state mass ($M = E_1 + E_2$)
μ_R - relativistic reduced mass:

$$\mu_R = \frac{E_1 E_2}{E_1 + E_2} = \frac{M^4 - (m_1^2 - m_2^2)^2}{4M^3}$$

$b(M)$ - on-mass-shell relative momentum in cms:

$$b^2(M) = \frac{[M^2 - (m_1 + m_2)^2][M^2 - (m_1 - m_2)^2]}{4M^2}$$

$E_{1,2}$ - center-of-mass energies:

$$E_1 = \frac{M^2 - m_2^2 + m_1^2}{2M}, \quad E_2 = \frac{M^2 - m_1^2 + m_2^2}{2M}$$

- **Baryons in quark-diquark picture**

(qq)-interaction:

$$V_{qq} = \frac{1}{2} V_{q\bar{q}}$$

$$V_{q\bar{q}}(\mathbf{p},\mathbf{q};M) = \bar{u}_1(p)\bar{u}_2(-p)\left\{\frac{4}{3}\alpha_s D_{\mu\nu}(\mathbf{k})\gamma_1^\mu\gamma_2^\nu + V^V_{\rm conf}(\mathbf{k})\Gamma_1^\mu\Gamma_{2;\mu} + V^S_{\rm conf}(\mathbf{k})\right\}u_1(q)u_2(-q)$$

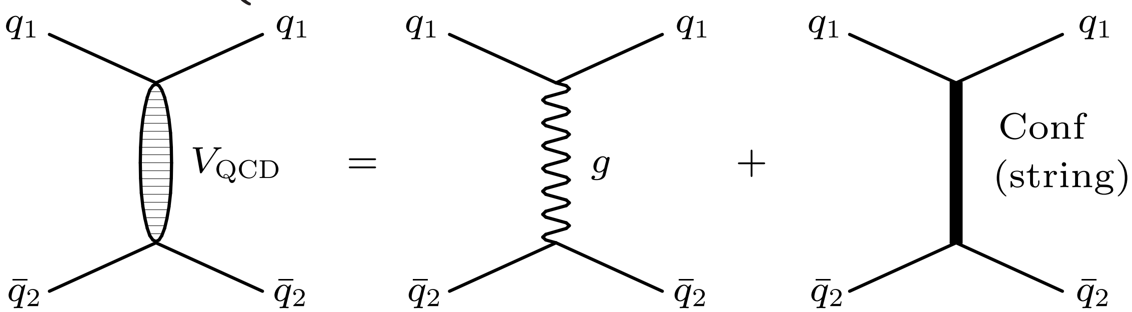

$\mathbf{k} = \mathbf{p} - \mathbf{q}$
$D_{\mu\nu}(\mathbf{k})$ - (perturbative) gluon propagator
$\Gamma_\mu(\mathbf{k})$ - effective long-range vertex with Pauli term:

$$\Gamma_\mu(\mathbf{k}) = \gamma_\mu + \frac{i\kappa}{2m}\sigma_{\mu\nu}k^\nu,$$

κ - anomalous chromomagnetic moment of quark,

$$u^\lambda(p) = \sqrt{\frac{\epsilon(p)+m}{2\epsilon(p)}}\begin{pmatrix} 1 \\ \dfrac{\boldsymbol{\sigma}\mathbf{p}}{\epsilon(p)+m}\end{pmatrix}\chi^\lambda, \qquad \epsilon(p) = \sqrt{\mathbf{p}^2+m^2}$$

.

- Lorentz structure of the quark potential

$$V_{\rm conf} = V_{\rm conf}^V + V_{\rm conf}^S$$

In nonrelativistic limit

$$\left.\begin{array}{rcl} V_{\rm conf}^V(r) & = & (1-\varepsilon)(Ar+B) \\ V_{\rm conf}^S(r) & = & \varepsilon(Ar+B) \end{array}\right\} \quad \text{Sum :} \quad (Ar+B)$$

ε - mixing parameter

$$V_{\rm NR}(r) = V_{\rm Coul}(r) + V_{\rm conf}(r) = -\frac{4}{3}\frac{\alpha_s}{r} + Ar + B$$

$$V_{\rm Coul}(r) = -\frac{4}{3}\frac{\alpha_s}{r}$$

(dQ)-interaction: $d = (qq')$

$$V(\mathbf{p},\mathbf{q};M) = \frac{\langle d(P)|J_\mu|d(Q)\rangle}{2\sqrt{E_d(p)E_d(q)}}\bar{u}_Q(p)\frac{4}{3}\alpha_s D_{\mu\nu}(\mathbf{k})\gamma^\nu u_Q(q)$$

$$+\psi_d^*(P)\bar{u}_Q(p)J_{d;\mu}\Gamma_Q^\mu V_{\rm conf}^V(\mathbf{k})u_Q(q)\psi_d(Q) + \psi_d^*(P)\bar{u}_Q(p)V_{\rm conf}^S(\mathbf{k})u_Q(q)\psi_d(Q)$$

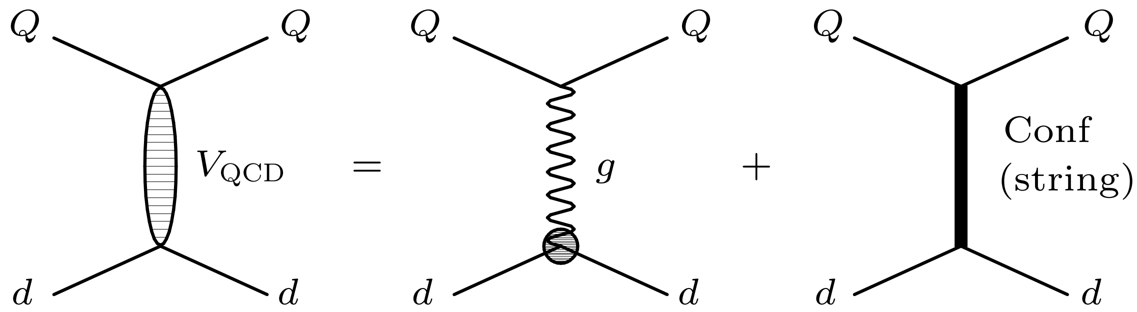

$J_{d,\mu}$ – effective long-range vector vertex of diquark:

$$J_{d;\mu} = \begin{cases} \dfrac{(P+Q)_\mu}{2\sqrt{E_d(p)E_d(q)}} & \text{for scalar diquark} \\[2ex] -\dfrac{(P+Q)_\mu}{2\sqrt{E_d(p)E_d(q)}} + \dfrac{i\mu_d}{2M_d}\Sigma_\mu^\nu k_\nu & \text{for axial vector diquark } (\mu_{\rm d}=0) \end{cases}$$

μ_d - total chromomagnetic moment of axial vector diquark

diquark spin matrix: $(\Sigma_{\rho\sigma})_\mu^\nu = -i(g_{\mu\rho}\delta_\sigma^\nu - g_{\mu\sigma}\delta_\rho^\nu)$

$\mathbf{S}_d$ - axial vector diquark spin: $(S_{d;k})_{il} = -i\varepsilon_{kil}$

$\psi_d(P)$ – diquark wave function:

$$\psi_d(p) = \begin{cases} 1 & \text{for scalar diquark} \\ \varepsilon_d(p) & \text{for axial vector diquark} \end{cases}$$

$\varepsilon_d(p)$ – polarization vector of axial vector diquark

Vertex of diquark-gluon interaction:

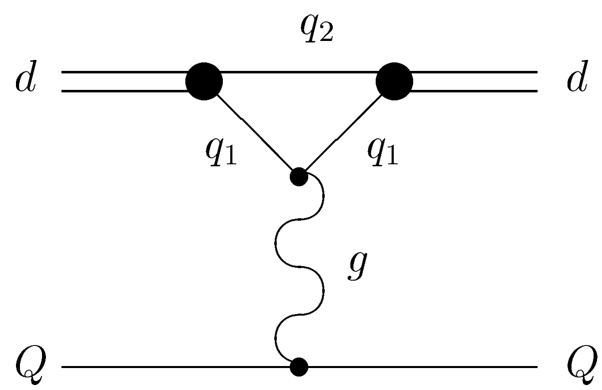

$$\langle d(P)|J_\mu(0)|d(Q)\rangle = \int \frac{d^3p\, d^3q}{(2\pi)^6} \bar{\Psi}^d_P(\mathbf{p})\Gamma_\mu(\mathbf{p},\mathbf{q})\Psi^d_Q(\mathbf{q}) \Rightarrow F(k^2)$$

Γ_μ – two-particle vertex function of the diquark-gluon interaction

The diquark-gluon interaction form factor can be parameterized by

$$F(r) = 1 - e^{-\xi r - \zeta r^2}$$

- Parameters of the model

Parameters A, B, κ, ε and quark masses fixed from analysis of meson masses and radiative decays:

$\varepsilon = -1$ from heavy quarkonium radiative decays $(J/\psi \to \eta_c + \gamma)$ and HQET

$\kappa = -1$ from fine splitting of heavy quarkonium ${}^3P_J$ states and HQET

$(1+\kappa) = 0 \Longrightarrow$ vanishing long-range chromomagnetic interaction ! (flux tube model)

Freezing of α_s

$$\alpha_s(\mu) = \frac{4\pi}{\beta_0 \ln \frac{\mu^2+M_0^2}{\Lambda^2}}, \quad \beta_0 = 11 - \frac{2}{3}n_f, \quad \mu = \frac{2m_1m_2}{m_1+m_2},$$

$$M_0 = 2.24\sqrt{A} = 0.95 \text{ GeV}$$

Quasipotential parameters:

$A = 0.18$ GeV^2, $B = -0.30$ GeV,

$\Lambda = 0.413$ GeV (from M_ρ)

Quark masses:

$m_b = 4.88$ GeV $m_s = 0.50$ GeV

$m_c = 1.55$ GeV $m_{u,d} = 0.33$ GeV

MASSES OF BARYONS

Quark-diquark picture of heavy and strange baryons reduces relativistic three-body problem to two step two-body calculation:

First step

- Masses and form factors of light diquarks are calculated

— Only ground-state scalar and axial vector diquarks are required for heavy baryons

— Ground-state, first orbital and radial excitations of light diquarks are necessary for strange baryons

Second step

- Heavy baryon is considered as a bound heavy-quark–light-diquark state

— All excitations are assumed to occur between heavy quark and light diquark

- In strange baryons two quarks of the same mass are assumed to form diquark

— Both excitations in quark-diquark system and lowest excitations of light diquark are considered

- Significantly less excited states than in genuine three-quark picture

Light diquarks

Table 1: Masses of light ground state diquarks (in MeV)

Quark content	Diquark type	Mass: our	NJL	BSE	BSE	Lattice
$[u,d]$	S	710	705	737	820	694(22)
$\{u,d\}$	A	909	875	949	1020	806(50)
$[u,s]$	S	948	895	882	1100	
$\{u,s\}$	A	1069	1050	1050	1300	
$\{s,s\}$	A	1203	1215	1130	1440	

Table 2: Masses M and form factor parameters of diquarks.

Quark content	I	State nl_j	M (MeV)	ξ (GeV)	ζ (GeV^2)
ud	0	$1s_0$	710	1.09	0.185
	1	$1s_1$	909	1.185	0.365
	0	$1p_0$	1321	1.395	0.148
	0	$1p_1$	1397	1.452	0.195
	0	$1p_2$	1475	1.595	0.173
	1	$1p_1$	1392	1.451	0.194
	0	$2s_0$	1513	1.01	0.055
	1	$2s_1$	1630	1.05	0.151
ss	0	$1s_1$	1203	1.13	0.280
	0	$1p_1$	1608	1.03	0.208
	0	$2s_1$	1817	0.805	0.235

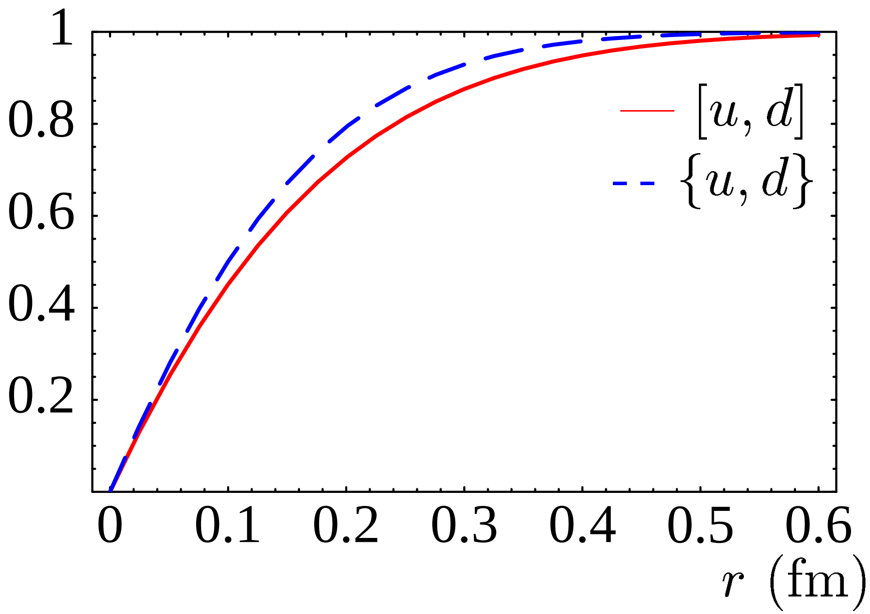

Figure 1: Form factors $F(r)$ for scalar $[u,d]$ (solid line) and axial vector $\{u,d\}$ (dashed line) diquarks.

Heavy and strange baryons

We do not expand the potential of the quark–diquark interaction either in p/m_Q or in p/m_d and treat both diquark and quark fully relativistically.
The resulting quasipotential of Qd interaction is extremely nonlocal in configuration space.
To simplify the potential and to make it local in configuration space we replace:

- the diquark energies

$$E_d(p) \equiv \sqrt{\mathbf{p}^2 + M_d^2} \to E_d = \frac{M^2 - m_Q^2 + M_d^2}{2M},$$

- the quark energies

$$\epsilon_Q(p) \equiv \sqrt{\mathbf{p}^2 + m_Q^2} \to E_Q = \frac{M^2 - M_d^2 + m_Q^2}{2M}.$$

These substitutions make the Fourier transform of the potential local, but introduce a complicated nonlinear dependence of the potential on the baryon mass M through the on-mass-shell energies E_d and E_Q.

The resulting Qd potential

$$V(r) = V_{\rm SI}(r) + V_{\rm SD}(r),$$

where $V_{\rm SI}(r)$ is the spin-independent part, and the structure of the spin-dependent potential is given by

$$V_{\rm SD}(r) = a_1\, \mathbf{L}\mathbf{S}_d + a_2\, \mathbf{L}\mathbf{S}_Q + b\left[-\mathbf{S}_d\mathbf{S}_Q + \frac{3}{r^2}(\mathbf{S}_d\mathbf{r})(\mathbf{S}_Q\mathbf{r})\right] + c\,\mathbf{S}_d\mathbf{S}_Q,$$

where $\mathbf{L}$ is the orbital angular momentum, $\mathbf{S}_d$ and $\mathbf{S}_Q$ are the diquark and quark spin operators, respectively. The coefficients a_1, a_2, b and c are expressed through the corresponding derivatives of the smeared Coulomb and confining potentials, e.g.:

$$c = \frac{2}{3}\frac{1}{E_d E_Q}\left\{\Delta\hat{V}_{\rm Coul}(r) - \frac{\mu_d}{2}\frac{E_d}{M_d}\left[\frac{E_Q - m_Q}{2m_Q} - (1+\kappa)\frac{E_Q + m_Q}{2m_Q}\right]\Delta V^V_{\rm conf}(r)\right\}.$$

The smeared Coulomb potential which accounts for the diquark internal structure

$$\hat{V}_{\rm Coul}(r) = -\frac{4}{3}\alpha_s\frac{F(r)}{r}.$$

Heavy baryons

Table 3: Masses of the ground state heavy baryons (in MeV). our – EFG, Phys. Rev. D (2005)

Baryon	$I(J^P)$	Theory						Experiment
		our (2005)	Capstick Isgur	Roncaglia et al.	Savage	Jenkins	Mathur* et al.	PDG
Λ_c	$0(\frac{1}{2}^+)$	2286	2265	2285			2290	2286.46(14)
Σ_c	$1(\frac{1}{2}^+)$	2443	2440	2453			2452	2453.76(18)
Σ_c^*	$1(\frac{3}{2}^+)$	2519	2495	2520	2518		2538	2518.0(0.5)
Ξ_c	$\frac{1}{2}(\frac{1}{2}^+)$	2476		2468			2473	$2470.88(^{34}_{80})$
Ξ_c'	$\frac{1}{2}(\frac{1}{2}^+)$	2579		2580	2579	2580.8(2.1)	2599	2577.9(2.9)
Ξ_c^*	$\frac{1}{2}(\frac{3}{2}^+)$	2649		2650			2680	2645.9(0.5)
Ω_c	$0(\frac{1}{2}^+)$	2698		2710			2678	2695.2(1.7)
Ω_c^*	$0(\frac{3}{2}^+)$	2768		2770	2768	2760.5(4.9)	2752	2765.9(2.0)
Λ_b	$0(\frac{1}{2}^+)$	5620	5585	5620			5672	5619.51(23)
Σ_b	$1(\frac{1}{2}^+)$	5808	5795	5820		5824.2(9.0)	5847	5811.3(1.9)
Σ_b^*	$1(\frac{3}{2}^+)$	5834	5805	5850		5840.0(8.8)	5871	5832.1(1.9)
Ξ_b	$\frac{1}{2}(\frac{1}{2}^+)$	5803		5810		5805.7(8.1)	5788	5794.4(1.2)
Ξ_b'	$\frac{1}{2}(\frac{1}{2}^+)$	5937		5950		5950.9(8.5)	5936	5935.02(5)
Ξ_b^*	$\frac{1}{2}(\frac{3}{2}^+)$	5963		5980		5966.1(8.3)	5959	5955.33(13)
Ω_b	$0(\frac{1}{2}^+)$	6064		6060		6068.7(11.1)	6040	6048.0(1.9)
Ω_b^*	$0(\frac{3}{2}^+)$	6088		6090		6083.2(11.0)	6060	

* error estimates of lattice calculations — ∼50 MeV for charmed, ∼100 MeV for bottom baryons

Table 4: Masses M of the Λ_Q ($Q = c, b$) heavy baryons (in MeV).

$I(J^P)$	Qd state	$Q=c$ M	status	$M^{\exp}$	$Q=b$ M	status	$M^{\exp}$
$0(\frac{1}{2}^+)$	$1S$	2286	****	2286.46(14)	5620	***	5619.51(23)
	$2S$	2769	*	2766.6(2.4)?	6089		
	$3S$	3130			6455		
	$4S$	3437			6756		
	$5S$	3715			7015		
	$6S$	3973			7256		
$0(\frac{1}{2}^-)$	$1P$	2598	***	2592.25(28)	5930	***	5912.11(26)
	$2P$	2983	***	2939.3$(^{1.4}_{1.5})$?	6326		
	$3P$	3303			6645		
	$4P$	3588			6917		
	$5P$	3852			7157		
$0(\frac{3}{2}^-)$	$1P$	2627	***	2628.1(6)	5942	***	5919.81(23)
	$2P$	3005			6333		
	$3P$	3322			6651		
	$4P$	3606			6922		
	$5P$	3869			7171		
$0(\frac{3}{2}^+)$	$1D$	2874			6190		
	$2D$	3189			6526		
	$3D$	3480			6811		
	$4D$	3747			7060		

Table 4: (continued)

$I(J^P)$	Qd state	$Q=c$ M	status	$M^{\rm exp}$	$Q=b$ M	status	$M^{\rm exp}$
$0(\frac{5}{2}^+)$	$1D$	2880	***	2881.53(35)	6196		
	$2D$	3209			6531		
	$3D$	3500			6814		
	$4D$	3767			7063		
$0(\frac{5}{2}^-)$	$1F$	3097			6408		
	$2F$	3375			6705		
	$3F$	3646			6964		
	$4F$	3900			7196		
$0(\frac{7}{2}^-)$	$1F$	3078			6411		
	$2F$	3393			6708		
	$3F$	3667			6966		
	$4F$	3922			7197		
$0(\frac{7}{2}^+)$	$1G$	3270			6598		
	$2G$	3546			6867		
$0(\frac{9}{2}^+)$	$1G$	3284			6599		
	$2G$	3564			6868		
$0(\frac{9}{2}^-)$	$1H$	3444			6767		
$0(\frac{11}{2}^-)$	$1H$	3460			6766		

Table 5: Comparison of theoretical predictions for masses of the Λ_c baryons (in MeV).

J^P	Experiment			Theory			
	State	Status	Mass	our	Chen et al.	Roberts Pervin	Capstick Isgur
$\frac{1}{2}^+$	Λ_c	***	2286.46	2286	2286	2286	2265
	$\Lambda_c(2765)$	*	2766.6	2769	2766	2791	2775
				3130	3112	3154	3170
				3437	3397		
$\frac{1}{2}^-$	$\Lambda_c(2595)$	***	2592.3	2598	2591	2625	2630
	$\Lambda_c(2940)$	***	2939.3	2983	2989		2780
				3303	3296		2830
$\frac{3}{2}^-$	$\Lambda_c(2625)$	***	2628.1	2627	2629	2636	2640
				3005	3000		2840
				3322	3301		2885
$\frac{3}{2}^+$				2874	2857	2887	2910
				3189	3188	3120	3035
$\frac{5}{2}^+$	$\Lambda_c(2880)$	***	2881.53	2880	2879	2887	2910
				3209	3198	3125	3140
$\frac{5}{2}^-$				3097	3075	2872	2900
$\frac{7}{2}^-$				3078	3092		3125
$\frac{7}{2}^+$				3270	3267		3175
$\frac{9}{2}^+$				3284	3280		

Strange baryons

Table 6: Masses of the ground states of hyperons (in MeV).

J^P	Experiment			Theory					
	State	Status	Mass	Our	Capstick Isgur	Loring et al.	Melde et al.	Santopinto Ferretti	Engel et al.
$\frac{1}{2}^+$	Λ	****	1115.683(6)	1115	1115	1108	1136	1116	1149(18)
$\frac{1}{2}^+$	Σ	****	1189.37(7)	1187	1190	1190	1180	1211	1216(15)
$\frac{3}{2}^+$	$\Sigma(1385)$	****	1382.80(35)	1381	1370	1411	1389	1334	1471(23)
$\frac{1}{2}^+$	Ξ	****	1321.71(7)	1330	1305	1310	1348	1317	1303(13)
$\frac{3}{2}^+$	$\Xi(1530)$	****	1531.80(32)	1518	1505	1539	1528	1552	1553(18)
$\frac{3}{2}^+$	Ω	****	1672.45(29)	1678	1635	1636	1672		1642(17)

Table 7: Masses of the positive parity Λ states (in MeV).

J^P	Experiment			Theory					
	State	Status	Mass	Our	Capstick Isgur	Loring et al.	Melde et al.	Santopinto Ferretti	Engel et al.
$\frac{1}{2}^+$	Λ	****	1115.683(6)	1115	1115	1108	1136	1116	1149(18)
	$\Lambda(1600)$	***	1560-1600	1615	1680	1677	1625	1518	1807(94)
	$\Lambda(1710)$	*	1713(13)						
	$\Lambda(1810)$	***	1750-1810	1901	1830	1747	1799	1666	2112(54)
				1972	1910	1898		1955	2137(69)
				1986	2010	2077		1960	
				2042	2105	2099			
				2099	2120	2132			
$\frac{3}{2}^+$	$\Lambda(1890)$	****	1850-1890	1854	1900	1823		1896	1991(103)
				1976	1960	1952			2058(139)
				2130	1995	2045			2481(111)
				2184	2050	2087			
				2202	2080	2133			
$\frac{5}{2}^+$	$\Lambda(1820)$	****	1815-1820	1825	1890	1834		1896	
	$\Lambda(2110)$	***	2090-2110	2098	2035	1999			
				2221	2115	2078			
				2255	2115	2127			
				2258	2180	2150			
$\frac{7}{2}^+$	$\Lambda(2020)$	*	$\approx$2020	2251	2120	2130			
				2471		2331			
$\frac{9}{2}^+$	$\Lambda(2350)$	***	2340-2350	2360		2340			

Table 8: Masses of the negative parity Λ states (in MeV).

J^P	Experiment			Theory					
	State	Status	Mass	Our	Capstick Isgur	Loring et al.	Melde et al.	Santopinto Ferretti	Engel et al.
$\frac{1}{2}^-$	$\Lambda(1405)$	****	$1405.1\binom{1.3}{1.0}$	1406	1550	1524	1556	1431	1416(81)
	$\Lambda(1670)$	****	1660-1670	1667	1615	1630	1682	1443	1546(110)
	$\Lambda(1800)$	***	1720-1800	1733	1675	1816	1778	1650	1713(116)
				1927	2015	2011		1732	2075(249)
				2197	2095	2076		1785	
				2218	2160	2117		1854	
$\frac{3}{2}^-$	$\Lambda(1520)$	****	1519.5(1.0)	1549	1545	1508	1556	1431	1751(40)
	$\Lambda(1690)$	****	1685-1690	1693	1645	1662	1682	1443	2203(106)
				1812	1770	1775		1650	2381(87)
	$\Lambda(2050)$	*	2056(22)	2035	2030	1987		1732	
				2319	2110	2090		1785	
	$\Lambda(2325)$	*	≈2325	2322	2185	2147		1854	
				2392	2230	2259		1928	
				2454	2290	2275		1969	
				2468		2313			
$\frac{5}{2}^-$	$\Lambda(1830)$	****	1810-1830	1861	1775	1828	1778	1785	
				2136	2180	2080			
				2350	2250	2179			
$\frac{7}{2}^-$	$\Lambda(2100)$	****	2090-2100	2097	2150	2090			
				2583	2230	2227			
$\frac{9}{2}^-$				2665		2370			

Table 9: Masses of the positive parity Σ states (in MeV).

J^P	Experiment			Theory					
	State	Status	Mass	Our	Capstick Isgur	Loring et al.	Melde et al.	Santopinto Ferretti	Engel et al.
$\frac{1}{2}^+$	Σ	****	1189.37(7)	1187	1190	1190	1180	1211	1216(15)
	$\Sigma(1660)$	***	1630-1660	1711	1720	1760	1616	1546	2069(74)
	$\Sigma(1770)$	*	≈1770	1922	1915	1947	1911	1668	2149(66)
	$\Sigma(1880)$	*	≈1880	1983	1970	2009		1801	2335(63)
				2028	2005	2052			
				2180	2030	2098			
				2292	2105	2138			
				2472	2195				
$\frac{3}{2}^+$	$\Sigma(1385)$	****	1382.80(35)	1381	1370	1411	1389	1334	1471(23)
	$\Sigma(1730)$	*	1727(27)		1920	1896	1865	1439	
	$\Sigma(1840)$	*	≈1840	1862	1970	1961		1924	2194(81)
	$\Sigma(1940)$	*	1941(18)	2025	2010	2011			2250(79)
	$\Sigma(2080)$	**	≈2080	2076	2030	2044			2468(67)
				2096	2045	2062			
				2157	2085	2103			
				2186	2115	2112			
$\frac{5}{2}^+$	$\Sigma(1915)$	****	1900-1915	1991	1995	1956		2061	
	$\Sigma(2070)$	*	≈2070	2062	2030	2027			
				2221	2095	2071			
$\frac{7}{2}^+$	$\Sigma(2030)$	****	2025-2030	2033	2060	2070			
				2470	2125	2161			

Table 10: Masses of the negative parity Σ states (in MeV).

J^P	Experiment			Theory					
	State	Status	Mass	Our	Capstick Isgur	Loring et al.	Melde et al.	Santopinto Ferretti	Engel et al.
$\frac{1}{2}^-$	$\Sigma(1620)$	*	≈1620	1620	1630	1628	1677	1753	1603(38)
				1693	1675	1771	1736	1868	1718(58)
	$\Sigma(1750)$	***	1730-1750	1747	1695	1798	1759	1895	1730(34)
	$\Sigma(1900)$	*	1900(21)	2115	2110	2111			2478(104)
	$\Sigma(2000)$	*	≈2000	2198	2155	2136			
				2202	2165	2251			
				2289	2205	2264			
				2381	2260	2288			
$\frac{3}{2}^-$	$\Sigma(1580)$	*	≈1580						
	$\Sigma(1670)$	***	1665-1670	1706	1655	1669	1677	1753	1736(40)
				1731	1750	1728	1736	1868	1861(20)
	$\Sigma(1940)$	***	1900-1940	1856	1755	1781	1759	1895	2297(122)
				2175	2120	2139			2394(74)
				2203	2185	2171			
				2300	2200	2203			
$\frac{5}{2}^-$	$\Sigma(1775)$	****	1770-1775	1757	1755	1770	1736	1753	
				2214	2205	2174			
				2347	2250	2226			
$\frac{7}{2}^-$	$\Sigma(2100)$	*	≈2100	2259	2245	2236			
				2349		2285			
$\frac{9}{2}^-$				2289		2325			

Regge trajectories of heavy and strange baryons

(a) The (J, M^2) Regge trajectory:

$$J = \alpha M^2 + \alpha_0$$

(b) The (n_r, M^2) Regge trajectory:

$$n_r = \beta M^2 + \beta_0,$$

α, β – slopes
α_0, β_0 – intercepts.

Baryons:
$P = (-1)^{J-1/2}$ – natural parity
$P = (-1)^{J+1/2}$ – unnatural parity

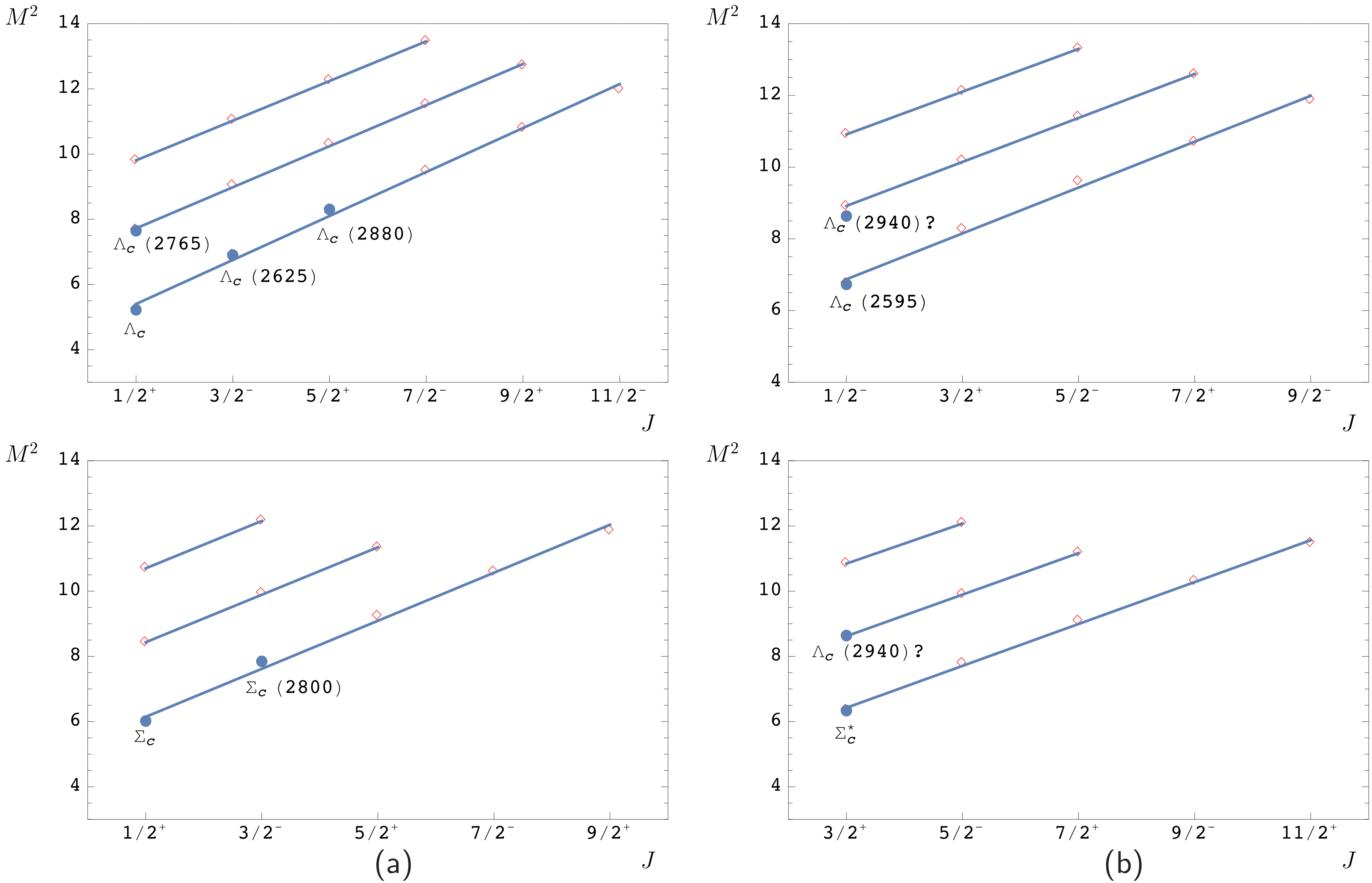

Figure 2: Parent and daughter (J, M^2) Regge trajectories for the Λ_c and Σ_c baryons with natural (a) and unnatural (b) parities. Diamonds are predicted masses. Available experimental data are given by dots with particle names; M^2 is in GeV^2.

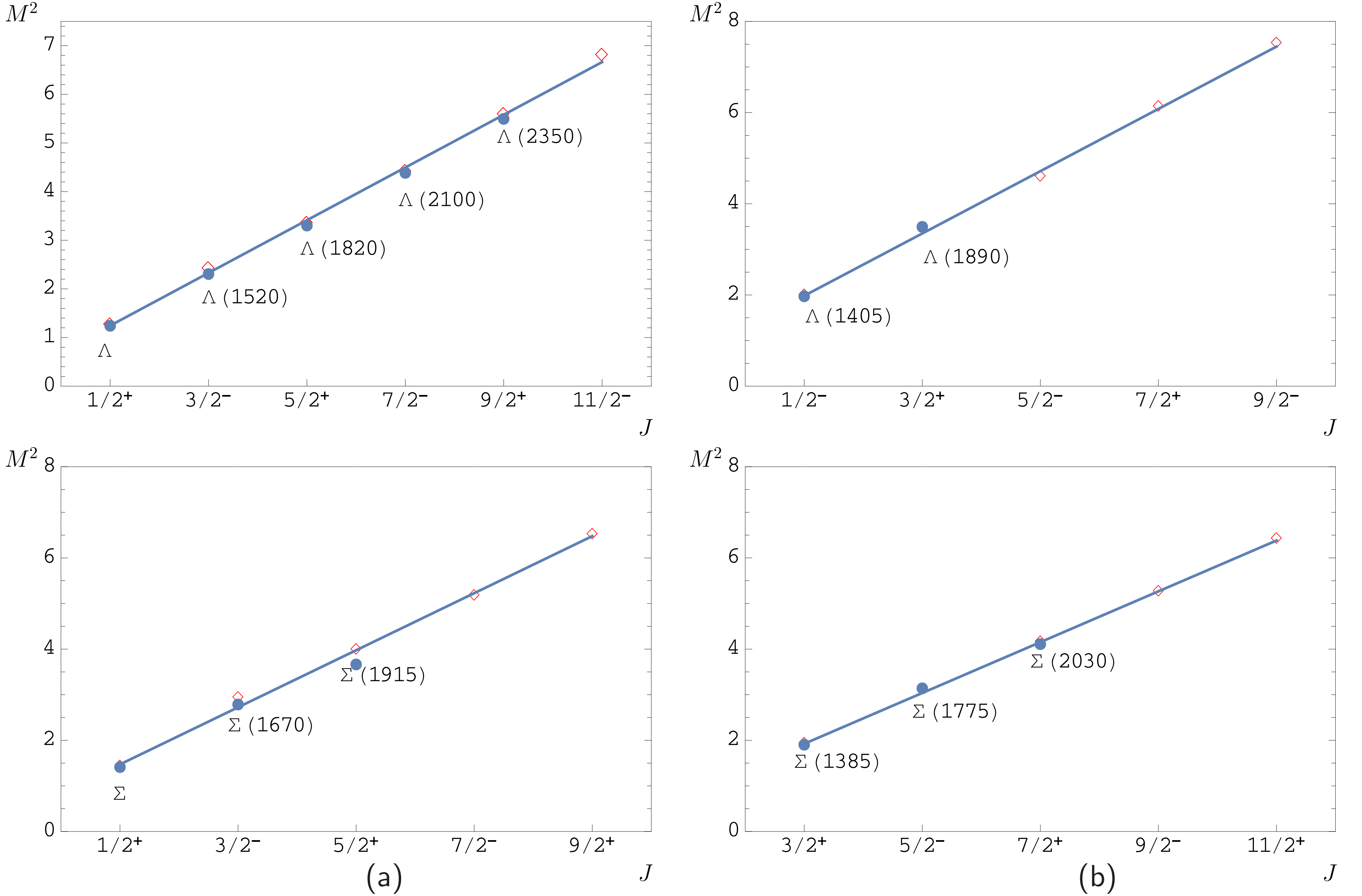

Figure 3: The (J, M^2) Regge trajectories for the Λ ans Σ baryons with natural (a) and unnatural (b) parities. Diamonds are predicted masses. Available experimental data are given by dots with particle names; M^2 is in GeV^2.

Table 11: Fitted parameters for the slope and intercept of the (J, M^2) parent and daughter Regge trajectories for heavy baryons with scalar and axial vector diquark.

Trajectory	α (GeV^{-2})	α_0	α (GeV^{-2})	α_0
$c[u,d]$	$\Lambda_c \left(\frac{1}{2}^+\right)$		$\Lambda_c \left(\frac{1}{2}^-\right)$	
parent	0.741 ± 0.024	-3.504 ± 0.205	0.782 ± 0.030	-4.874 ± 0.276
1 daughter	0.793 ± 0.013	-5.626 ± 0.129	0.815 ± 0.009	-6.769 ± 0.099
$c\{q,q\}$	$\Sigma_c \left(\frac{1}{2}^+\right)$		$\Sigma_c^* \left(\frac{3}{2}^+\right)$	
parent	0.679 ± 0.032	-3.670 ± 0.278	0.778 ± 0.019	-3.498 ± 0.164
1 daughter	0.686 ± 0.016	-5.289 ± 0.158	0.785 ± 0.001	-5.264 ± 0.012
$c[s,q]$	$\Xi_c \left(\frac{1}{2}^+\right)$		$\Xi_c \left(\frac{1}{2}^-\right)$	
parent	0.686 ± 0.025	-3.852 ± 0.240	0.728 ± 0.020	-5.249 ± 0.211
1 daughter	0.739 ± 0.015	-6.025 ± 0.169	0.764 ± 0.012	-7.244 ± 0.142
$c\{s,s\}$	$\Omega_c \left(\frac{1}{2}^+\right)$		$\Omega_c^* \left(\frac{3}{2}^+\right)$	
parent	0.615 ± 0.023	-4.065 ± 0.023	0.690 ± 0.020	-3.858 ± 0.205
1 daughter	0.565 ± 0.028	-4.910 ± 0.316	0.608 ± 0.012	-4.436 ± 0.133
$b[u,d]$	$\Lambda_b \left(\frac{1}{2}^+\right)$		$\Lambda_b \left(\frac{1}{2}^-\right)$	
parent	0.352 ± 0.017	-10.83 ± 0.65	0.376 ± 0.014	-12.82 ± 0.58
1 daughter	0.397 ± 0.015	-14.33 ± 0.64	0.419 ± 0.010	-16.33 ± 0.45
$b[s,q]$	$\Xi_b \left(\frac{1}{2}^+\right)$		$\Xi_b \left(\frac{1}{2}^-\right)$	
parent	0.349 ± 0.019	-11.49 ± 0.80	0.381 ± 0.014	-13.88 ± 0.60
1 daughter	0.399 ± 0.016	-15.27 ± 0.69	0.423 ± 0.011	-17.40 ± 0.49
$b\{s,s\}$	$\Omega_b \left(\frac{1}{2}^+\right)$		$\Omega_b^* \left(\frac{3}{2}^+\right)$	
parent	0.365 ± 0.013	-13.04 ± 0.58	0.389 ± 0.011	-13.02 ± 0.47
1 daughter	0.378 ± 0.052	-15.30 ± 2.35	0.401 ± 0.062	-15.33 ± 2.74

Table 12: Fitted parameters α, α_0 for the slope and intercept of the (J, M^2) Regge trajectories of strange baryons.

Baryon	α (GeV^{-2})	α_0	Baryon	α (GeV^{-2})	α_0
Λ $(\frac{1}{2}^+)$	0.923 ± 0.016	-0.648 ± 0.057	Λ $(\frac{1}{2}^-)$	0.732 ± 0.018	-0.951 ± 0.074
Σ $(\frac{1}{2}^+)$	0.799 ± 0.029	-0.676 ± 0.100	Σ $(\frac{3}{2}^+)$	0.897 ± 0.010	-0.225 ± 0.037
Ξ $(\frac{1}{2}^+)$	0.694 ± 0.007	-0.721 ± 0.024	Ξ $(\frac{3}{2}^+)$	0.769 ± 0.032	-0.249 ± 0.098
			Ω $(\frac{3}{2}^+)$	0.712 ± 0.002	-0.504 ± 0.007

The slopes of the heavy and strange baryon Regge trajectories follow in both planes the regularities previously observed for light and heavy mesons:

- decrease with the increase of the diquark mass
- decrease with the increase of the parent baryon mass

The latter decrease is significantly more pronounced.

The ratio of slopes for heavy baryons and heavy-light mesons:

$$\langle \alpha_{Qqq} \rangle / \langle \alpha_{Q\bar{q}} \rangle \sim \langle \beta_{Qqq} \rangle / \langle \beta_{Q\bar{q}} \rangle \sim 1.4$$

Strange baryons and strange mesons have almost equal values of the Regge slopes

SEMILEPTONIC DECAYS

- Heavy-to-heavy and heavy-to-light semileptonic decays of baryons: $B_Q \to B_{Q'} e\nu$ ($Q = b$, $Q' = c, u$)

Additional source for the determination of V_{cb} and V_{ub}.

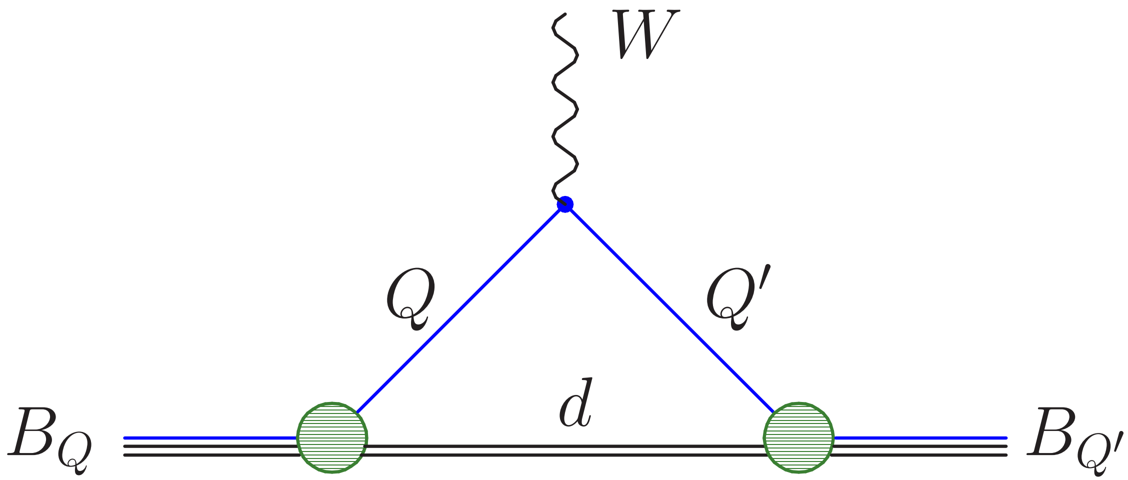

Active heavy quark and spectator light diquark.

• Matrix elements of weak current

Matrix element of weak current $J_\mu^W = \bar{Q}'\gamma_\mu(1-\gamma_5)Q$:

$$\langle B_{Q'}(P')|J_\mu^W|B_Q(P)\rangle = \int \frac{d^3p\, d^3q}{(2\pi)^6}\bar{\Psi}_{B_{Q'}\,\mathbf{P}'}(\mathbf{p})\Gamma_\mu(\mathbf{p},\mathbf{q})\Psi_{B_Q\,\mathbf{P}}(\mathbf{q}),$$

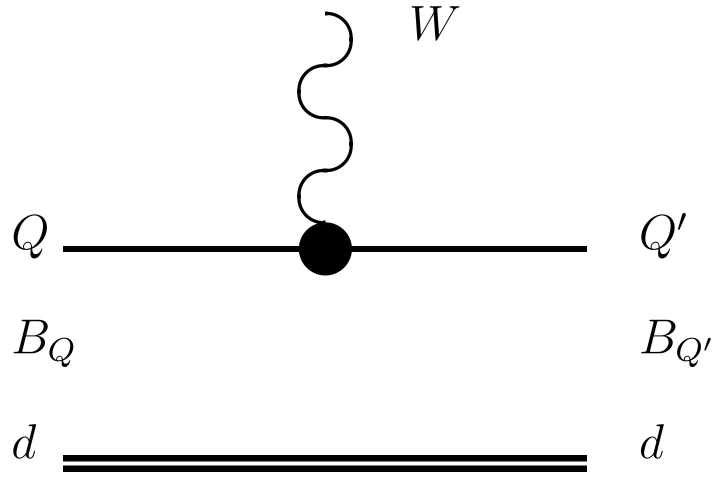

Figure 4: Lowest order vertex function $\Gamma^{(1)}$ contributing to the current matrix element.

$$\Gamma_\mu^{(1)}(\mathbf{p},\mathbf{q}) = \psi_d^*(p_d)\bar{u}_{Q'}(p_{Q'})\gamma_\mu(1-\gamma^5)u_Q(q_Q)\psi_d(q_d)(2\pi)^3\delta(\mathbf{p}_d-\mathbf{q}_d)$$

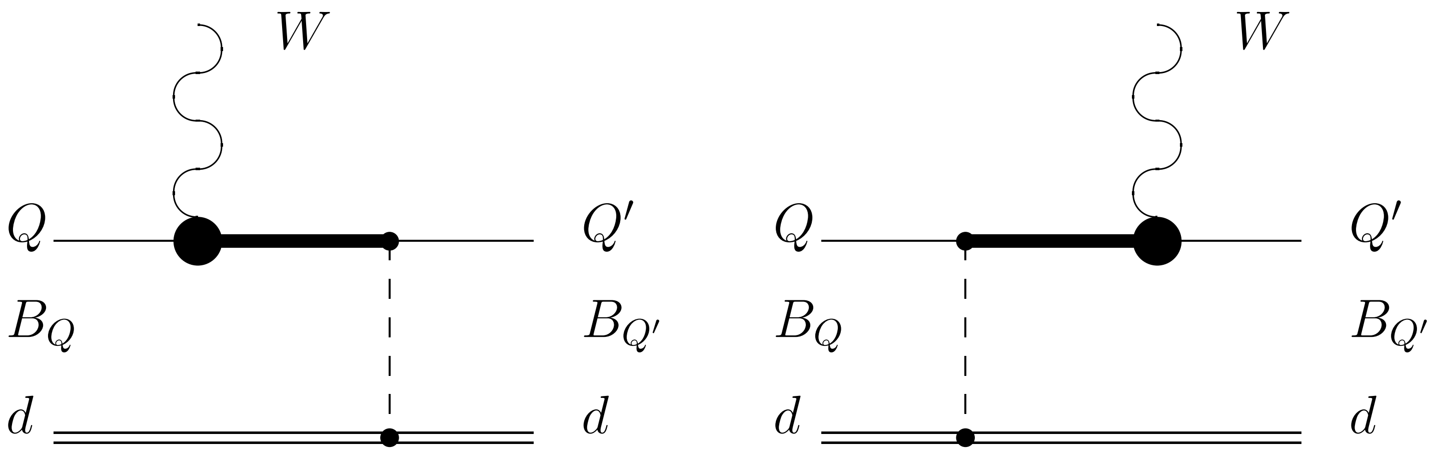

Figure 5: Vertex function $\Gamma^{(2)}$ taking the quark interaction into account. Dashed lines correspond to the effective potential $\mathcal{V}_{Qd}$. Bold lines denote the negative-energy part of the quark propagator.

$$
\begin{aligned}
\Gamma_\mu^{(2)}(\mathbf{p},\mathbf{q}) \quad = \quad & \psi_d^*(p_d)\bar{u}_{Q'}(p_{Q'})\Big\{\gamma_\mu(1-\gamma^5)\frac{\Lambda_Q^{(-)}(k)}{\epsilon_Q(k)+\epsilon_Q(p_{Q'})}\gamma^0\mathcal{V}_{Qd}(\mathbf{p}_d-\mathbf{q}_d) \\
& + \mathcal{V}_{Qd}(\mathbf{p}_d-\mathbf{q}_d)\frac{\Lambda_{Q'}^{(-)}(k')}{\epsilon_{Q'}(k')+\epsilon_{Q'}(q_Q)}\gamma^0\gamma_\mu(1-\gamma^5)\Big\}u_Q(q_Q)\psi_d(q_d),
\end{aligned}
$$

where

$$\Lambda^{(-)}(p) = \frac{\epsilon(p) - \big(m\gamma^0 + \gamma^0(\boldsymbol{\gamma}\mathbf{p})\big)}{2\epsilon(p)}$$

$\mathbf{k} = \mathbf{p}_{Q'} - \boldsymbol{\Delta};\ \mathbf{k}' = \mathbf{q}_Q + \boldsymbol{\Delta};\ \boldsymbol{\Delta} = \mathbf{P}' - \mathbf{P};\ \epsilon(p) = \sqrt{m^2 + \mathbf{p}^2}$

Wave function $\Psi_{B_{Q'}\mathbf{P}'}$ of the moving baryon is connected with the rest-frame wave function $\Psi_{B_{Q'}\mathbf{0}} \equiv \Psi_{B_{Q'}}$ by the transformation

$$\Psi_{B_{Q'}\mathbf{P}'}(\mathbf{p}) = D_{Q'}^{1/2}(R_{L_{\mathbf{P}'}}^{W}) D_{d}^{\mathcal{I}}(R_{L_{\mathbf{P}'}}^{W}) \Psi_{B_{Q'}\mathbf{0}}(\mathbf{p}), \qquad \mathcal{I} = 0, 1,$$

where R^W – Wigner rotation, $L_{\mathbf{P}'}$ – Lorentz boost from the baryon rest frame to a moving one.

- Rotation matrix $D_Q^{1/2}(R)$ of quark spin:

$$\begin{pmatrix} 1 & 0 \\ 0 & 1 \end{pmatrix} D_{Q'}^{1/2}(R_{L_{\mathbf{P}'}}^{W}) = S^{-1}(\mathbf{p}_{Q'}) S(\mathbf{P}') S(\mathbf{p}),$$

$$S(\mathbf{p}) = \sqrt{\frac{\epsilon(p)+m}{2m}} \left(1 + \frac{\boldsymbol{\alpha}\mathbf{p}}{\epsilon(p)+m}\right).$$

- Rotation matrix $D_d^{\mathcal{I}}(R)$ of diquark with spin $\mathcal{I} = 0, 1$:
  $D_d^0(R^W) = 1$ for scalar diquark
  $D_d^1(R^W) = R^W$ for axial vector diquark.

- heavy-to-heavy decays $\Lambda_b \to \Lambda_c l \nu_l$ $b \to c$ transition CKM favored V_{cb} $Br \sim 10^{-2}$
- heavy-to-light decays $\Lambda_b \to p l \nu_l$ $b \to u$ transition CKM suppressed V_{ub} $Br \sim 10^{-4}$

Broad kinematical range:
the square of momentum transfer to the lepton pair q^2 varies
from 0 to $q^2_{\max} \approx 10$ GeV^2 for decays to Λ_c
from 0 to $q^2_{\max} \approx 20$ GeV^2 for decays to p
$\Longrightarrow$ the explicit determination of the q^2 dependence of the decay form factors in the whole kinematical range is needed

Large recoil of the final baryon requires consistent relativistic treatment (e.g. boost of the baryon wave functions from the rest to the moving reference frame)

Presence of heavy quarks in Λ_b and Λ_c baryons allows one to use expansions in the inverse powers of heavy quark masses $1/m_{b,c} \Longrightarrow$ significant simplifications, heavy quark symmetry relations can be used

Light u, d, s quarks should be treated relativistically

Large recoils allow one to neglect small relative momentum ($|\mathbf{p}|$) with respect to recoil ($|\mathbf{\Delta}|$) in the energies of light quarks in energetic light baryons $\epsilon_q(p + \Delta) \equiv \sqrt{m_q^2 + (\mathbf{p} + \mathbf{\Delta})^2} \longrightarrow \epsilon_q(\Delta) \equiv \sqrt{m_q^2 + \mathbf{\Delta}^2}$.
Such replacement is made in subleading contribution $\Gamma_\mu^{(2)}(\mathbf{p}, \mathbf{q})$ and permits to perform one of the integrations using the quasipotential equation. As a result, the weak decay matrix element is expressed through the usual overlap integral of initial and final meson wave functions

Heavy-to-heavy semileptonic $\Lambda_b \to \Lambda_c$ decays

HQS ($m_Q \to \infty$):

heavy quark spin and mass decouple $\to$ heavy baryon properties are determined by light diquarks $\to$

- masses of ground state baryons with spin $1/2$ and $3/2$ containing the axial vector diquark are degenerate
- for $\Lambda_b \to \Lambda_c$ one universal form factor $\zeta(w)$ (Isgur-Wise function)
- for $\Omega_b \to \Omega_c$ two universal form factors $\zeta_1(w)$ and $\zeta_2(w)$
- isospin violating decay amplitudes, e.g. $\Lambda_b \to \Sigma_c$, vanish

$1/m_Q$ order:

- for $\Lambda_Q \to \Lambda_{Q'}$ one additional mass parameter $\bar{\Lambda}$ and one additional function $\chi(w)$
- for $\Omega_Q \to \Omega_{Q'}$ one additional mass parameter $\bar{\Lambda}$ and five additional functions

- **Form factors of heavy baryons with scalar diquark**

Hadronic matrix elements for $\Lambda_Q \to \Lambda_q e\nu$:

$$\langle \Lambda_q(p',s')|V^\mu|\Lambda_Q(p,s)\rangle = \bar u_{\Lambda_q}(p',s')\Big[F_1(q^2)\gamma^\mu + F_2(q^2)\frac{p^\mu}{M_{\Lambda_Q}} + F_3(q^2)\frac{p'^\mu}{M_{\Lambda_q}}\Big]u_{\Lambda_Q}(p,s),$$

$$\langle \Lambda_q(p',s')|A^\mu|\Lambda_Q(p,s)\rangle = \bar u_{\Lambda_q}(p',s')\Big[G_1(q^2)\gamma^\mu + G_2(q^2)\frac{p^\mu}{M_{\Lambda_Q}} + G_3(q^2)\frac{p'^\mu}{M_{\Lambda_q}}\Big]\gamma_5 u_{\Lambda_Q}(p,s),$$

An other popular parametrisation

$$\langle \Lambda_q(p',s')|V^\mu|\Lambda_Q(p,s)\rangle = \bar u_{\Lambda_q}(p',s')\Big[f_1^V(q^2)\gamma^\mu - f_2^V(q^2)i\sigma^{\mu\nu}\frac{q_\nu}{M_{\Lambda_Q}} + f_3^V(q^2)\frac{q^\mu}{M_{\Lambda_Q}}\Big]u_{\Lambda_Q}(p,s),$$

$$\langle \Lambda_q(p',s')|A^\mu|\Lambda_Q(p,s)\rangle = \bar u_{\Lambda_q}(p',s')[f_1^A(q^2)\gamma^\mu - f_2^A(q^2)i\sigma^{\mu\nu}\frac{q_\nu}{M_{\Lambda_Q}} + f_3^A(q^2)\frac{q^\mu}{M_{\Lambda_Q}}\Big]\gamma_5 u_{\Lambda_Q}(p,s)$$

Relations

$$f_1^V(q^2) = F_1(q^2) + (M_{\Lambda_Q}+M_{\Lambda_q})\left[\frac{F_2(q^2)}{2M_{\Lambda_Q}} + \frac{F_3(q^2)}{2M_{\Lambda_q}}\right],$$

$$f_2^V(q^2) = -\frac{1}{2}\left[F_2(q^2) + \frac{M_{\Lambda_Q}}{M_{\Lambda_q}}F_3(q^2)\right], \qquad f_3^V(q^2) = \frac{1}{2}\left[F_2(q^2) - \frac{M_{\Lambda_Q}}{M_{\Lambda_q}}F_3(q^2)\right],$$

$$f_1^A(q^2) = G_1(q^2) - (M_{\Lambda_Q}-M_{\Lambda_q})\left[\frac{G_2(q^2)}{2M_{\Lambda_Q}} + \frac{G_3(q^2)}{2M_{\Lambda_q}}\right],$$

$$f_2^A(q^2) = -\frac{1}{2}\left[G_2(q^2) + \frac{M_{\Lambda_Q}}{M_{\Lambda_q}}G_3(q^2)\right], \qquad f_3^A(q^2) = \frac{1}{2}\left[G_2(q^2) - \frac{M_{\Lambda_Q}}{M_{\Lambda_q}}G_3(q^2)\right].$$

- **Heavy quark expansion**

- In heavy quark limit $m_Q \to \infty$

$$F_1(w) = G_1(w) = \zeta(w), \qquad F_2(w) = F_3(w) = G_2(w) = G_3(w) = 0,$$

$$w = v \cdot v' = \frac{M^2_{\Lambda_Q} + M^2_{\Lambda_{Q'}} - q^2}{2M_{\Lambda_Q} M_{\Lambda_{Q'}}}.$$

- At $1/m_Q$ order in HQET

$$F_1(w) = \zeta(w) + \left(\frac{\bar{\Lambda}}{2m_Q} + \frac{\bar{\Lambda}}{2m_{Q'}}\right)\left[2\chi(w) + \zeta(w)\right],$$

$$G_1(w) = \zeta(w) + \left(\frac{\bar{\Lambda}}{2m_Q} + \frac{\bar{\Lambda}}{2m_{Q'}}\right)\left[2\chi(w) + \frac{w-1}{w+1}\zeta(w)\right],$$

$$F_2(w) = G_2(w) = -\frac{\bar{\Lambda}}{2m_{Q'}}\frac{2}{w+1}\zeta(w), \qquad F_3(w) = -G_3(w) = -\frac{\bar{\Lambda}}{2m_Q}\frac{2}{w+1}\zeta(w).$$

In our model up to $1/m_Q$ order

$$F_1(w) = \zeta(w) + \left(\frac{\bar\Lambda}{2m_Q} + \frac{\bar\Lambda}{2m_{Q'}}\right)[2\chi(w) + \zeta(w)]$$
$$+4(1-\varepsilon)(1+\kappa)\left[\frac{\bar\Lambda}{2m_{Q'}}\frac{1}{w-1} - \frac{\bar\Lambda}{2m_Q}(w+1)\right]\chi(w),$$
$$G_1(w) = \zeta(w) + \left(\frac{\bar\Lambda}{2m_Q} + \frac{\bar\Lambda}{2m_{Q'}}\right)\left[2\chi(w) + \frac{w-1}{w+1}\zeta(w)\right] - 4(1-\varepsilon)(1+\kappa)\frac{\bar\Lambda}{2m_Q}w\chi(w),$$
$$F_2(w) = -\frac{\bar\Lambda}{2m_{Q'}}\frac{2}{w+1}\zeta(w) - 4(1-\varepsilon)(1+\kappa)\left[\frac{\bar\Lambda}{2m_{Q'}}\frac{1}{w-1} + \frac{\bar\Lambda}{2m_Q}w\right]\chi(w),$$
$$G_2(w) = -\frac{\bar\Lambda}{2m_{Q'}}\frac{2}{w+1}\zeta(w) - 4(1-\varepsilon)(1+\kappa)\frac{\bar\Lambda}{2m_{Q'}}\frac{1}{w-1}\chi(w),$$
$$F_3(w) = -G_3(w) = -\frac{\bar\Lambda}{2m_Q}\frac{2}{w+1}\zeta(w) + 4(1-\varepsilon)(1+\kappa)\frac{\bar\Lambda}{2m_Q}\chi(w).$$

⋆ For $(1-\varepsilon)(1+\kappa) = 0$ HQET results are reproduced ($\kappa = -1$ in our model)!

- Leading order Isgur-Wise function ($\mathbf{e}_{\boldsymbol{\Delta}} = \boldsymbol{\Delta}/\sqrt{\boldsymbol{\Delta}^2}$)

$$\zeta(w) = \lim_{m_Q\to\infty} \int \frac{d^3p}{(2\pi)^3} \Psi_{\Lambda_{Q'}}\left(\mathbf{p} + 2\epsilon_d(p)\sqrt{\frac{w-1}{w+1}}\,\mathbf{e}_{\boldsymbol{\Delta}} \right) \Psi_{\Lambda_Q}(\mathbf{p}).$$

- Subleading function (very small)

$$\chi(w) = -\frac{w-1}{w+1} \lim_{m_Q\to\infty} \int \frac{d^3p}{(2\pi)^3} \Psi_{\Lambda_{Q'}}\left(\mathbf{p} + 2\epsilon_d(p)\sqrt{\frac{w-1}{w+1}}\,\mathbf{e}_{\boldsymbol{\Delta}} \right) \frac{\bar{\Lambda} - \epsilon_d(p)}{2\bar{\Lambda}} \Psi_{\Lambda_Q}(\mathbf{p}).$$

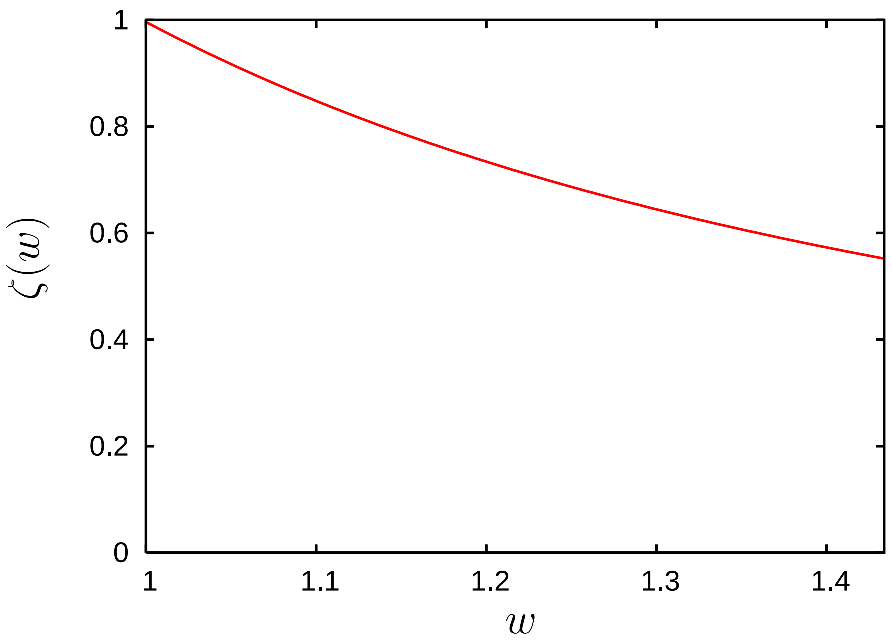

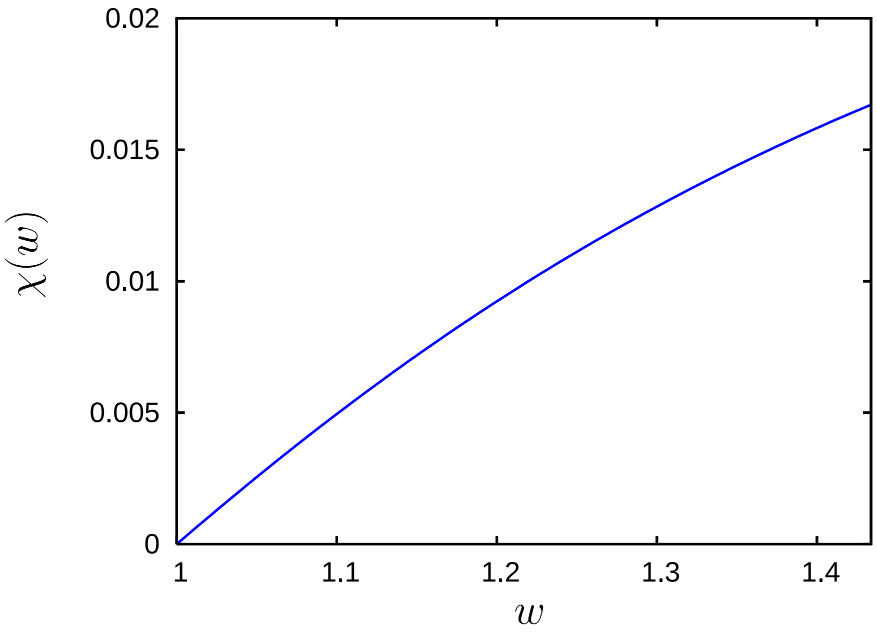

Table 13: Comparison of different theoretical predictions for semileptonic decay rates Γ (in $10^{10}\mathrm{s}^{-1}$) of bottom baryons.

Decay	Our RQM	Singleton NRQM	Cheng NRQM	Körner NRQM	Ivanov RTQM	Ivanov BS	Cardarelli LF	Albertus NRQM	Huang sum rule
$\Lambda_b \to \Lambda_c e\nu$	5.10	5.9	5.1	5.14	5.39	6.09	5.08 ± 1.3	5.82	5.4 ± 0.4
$\Xi_b \to \Xi_c e\nu$	5.03	7.2	5.3	5.21	5.27	6.42	5.68 ± 1.5	4.98	
$\Sigma_b \to \Sigma_c e\nu$	1.44	4.3			2.23	1.65			
$\Xi_b' \to \Xi_c' e\nu$	1.34								
$\Omega_b \to \Omega_c e\nu$	1.29	5.4	2.3	1.52	1.87	1.81			
$\Sigma_b \to \Sigma_c^* e\nu$	3.23				4.56	3.75			
$\Xi_b' \to \Xi_c^* e\nu$	3.09								
$\Omega_b \to \Omega_c^* e\nu$	3.03			3.41	4.01	4.13			

Our prediction for the branching ratio ($|V_{cb}| = 0.039$, $\tau_{\Lambda_b} = 1.466 \times 10^{-12}$s)

$$Br^{\rm theor}(\Lambda_b \to \Lambda_c l\nu) = 7.2\%$$

Experiment

$$Br^{\rm exp}(\Lambda_b \to \Lambda_c l\nu) = (6.2^{+1.4}_{-1.2})\%$$

Heavy-to-light semileptonic $\Lambda_b \to p$ decays

- **Without heavy quark expansion**

Large recoil:

$$|\mathbf{p}| \ll |\mathbf{\Delta}| \Longrightarrow \epsilon_q(p+\Delta) \equiv \sqrt{m_q^2 + (\mathbf{p}+\mathbf{\Delta})^2} \longrightarrow \epsilon_q(\Delta) \equiv \sqrt{m_q^2 + \mathbf{\Delta}^2}$$

in subleading contribution $\Gamma_\mu^{(2)}(\mathbf{p},\mathbf{q})$ and perform one of the integrations using the quasipotential equation.

$$F_i(q^2) = F_i^{(1)}(q^2) + \varepsilon F_i^{(2)S}(q^2) + (1-\varepsilon)F_i^{(2)V}(q^2)$$
$$G_i(q^2) = F_i^{(1)}(q^2) + \varepsilon G_i^{(2)S}(q^2) + (1-\varepsilon)G_i^{(2)V}(q^2) \qquad (i=1,2,3)$$

$$F_1^{(1)}(q^2) = \int \frac{d^3p}{(2\pi)^3}\bar{\Psi}_F\left(\mathbf{p} + \frac{2\epsilon_d}{E_F+M_F}\mathbf{\Delta}\right)\sqrt{\frac{\epsilon_Q(p)+m_Q}{2\epsilon_Q(p)}}\sqrt{\frac{\epsilon_q(p+\Delta)+m_q}{2\epsilon_q(p+\Delta)}}$$
$$\times\left\{1 + \frac{\epsilon_d}{\epsilon_q(p+\Delta)+m_q}\left[1 + \frac{\epsilon_d}{\epsilon_Q(p)+m_Q}\frac{E_F-M_F}{E_F+M_F}\right] + \frac{\epsilon_d}{\epsilon_Q(p)+m_Q}\right.$$
$$-\frac{1}{3}\frac{\mathbf{p}^2}{(\epsilon_q(p+\Delta)+m_q)(\epsilon_Q(p)+m_Q)} - \frac{\mathbf{p}\mathbf{\Delta}}{E_F+M_F}\left[\frac{1}{\epsilon_q(p+\Delta)+m_q}\right.$$
$$\left.\left.-\frac{1}{\epsilon_Q(p)+m_Q} + \frac{2M_F}{E_F+M_F}\frac{\epsilon_d}{(\epsilon_q(p+\Delta)+m_q)(\epsilon_Q(p)+m_Q)}\right]\right\}\Psi_I(\mathbf{p})$$

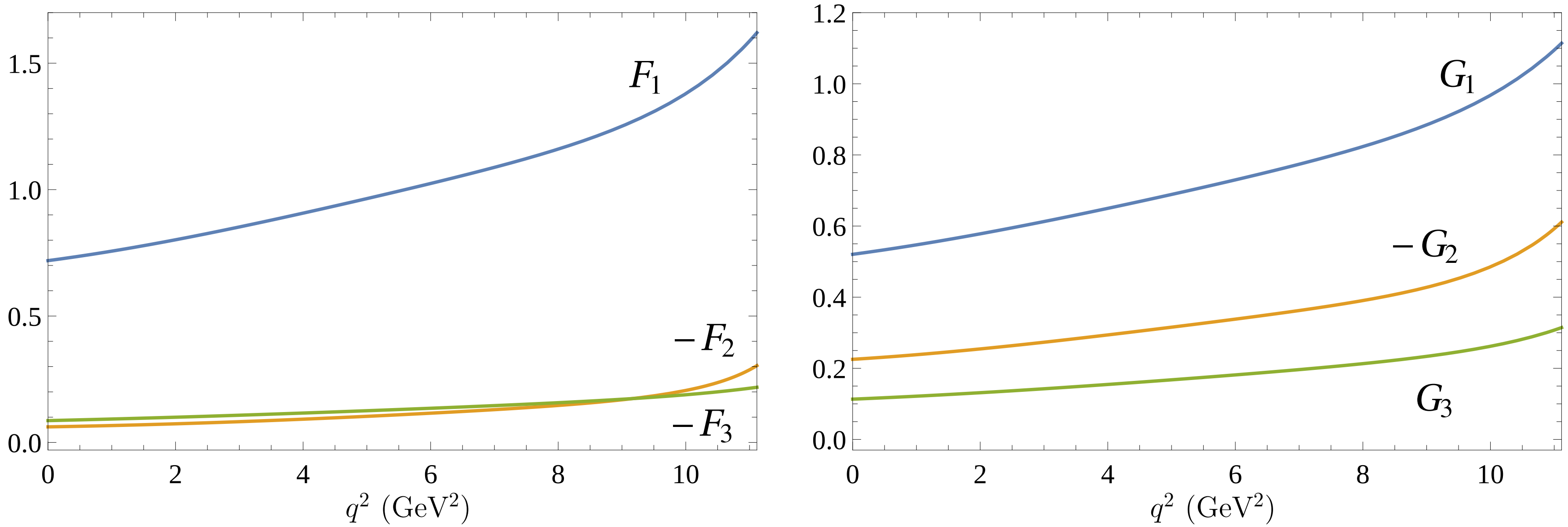

Figure 6: Form factors of the weak $\Lambda_b \to \Lambda_c$ transition.

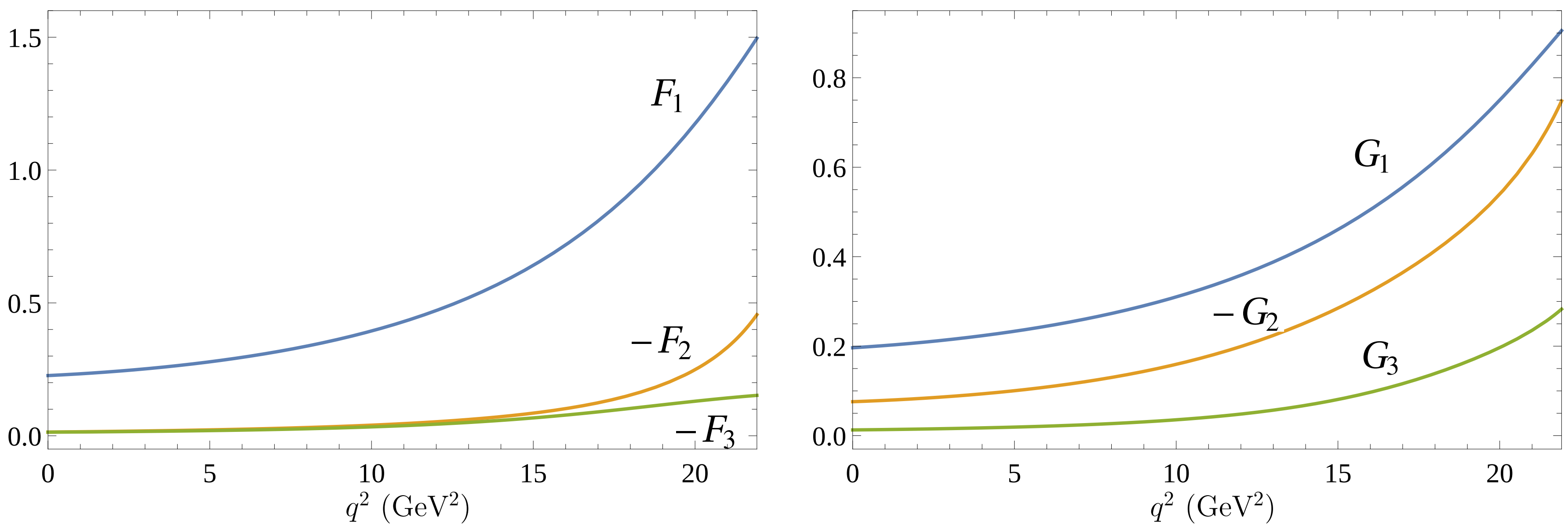

Figure 7: Form factors of the weak $\Lambda_b \to p$ transition.

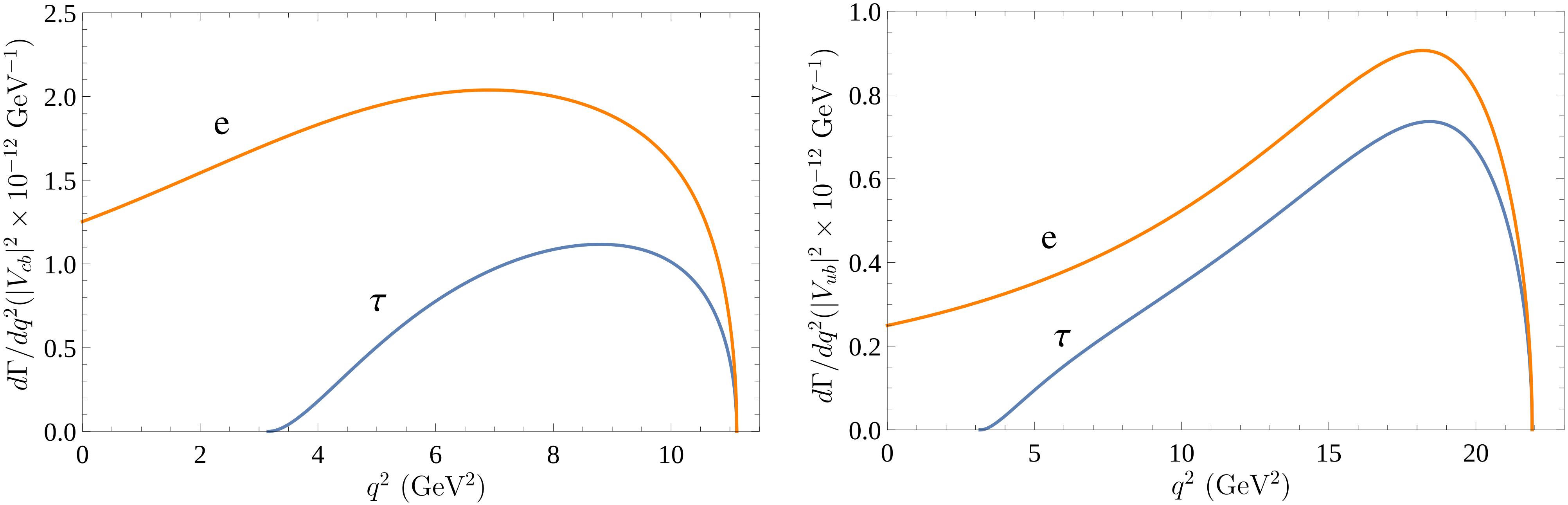

Figure 8: Predictions for the differential decay rates of the $\Lambda_b \to \Lambda_c l\nu$ (left) and $\Lambda_b \to pl\nu$ (right) semileptonic decays.

Table 14: Comparison of theoretical predictions for baryon semileptonic decay parameters with available experimental data.

Parameter	our RQM	Ivanov CCQM	Pervin SRQM	Dutta ELA	Ke LFQM	Detmold Lattice	Experiment PDG
$\Lambda_b \to \Lambda_c l\nu$							
Γ (ns^{-1})	44.2		53.9				
$\Gamma/\lvert V_{cb}\rvert^2$ (ps^{-1})	29.1					$21.5 \pm 0.8 \pm 1.1$	
Br (%)	6.48	6.9		4.83	6.3		$6.2^{+1.4}_{-1.2}$
$\Lambda_b \to \Lambda_c \tau\nu$							
Γ (ns^{-1})	13.9		20.9				
$\Gamma/\lvert V_{cb}\rvert^2$ (ps^{-1})	9.11					$7.15 \pm 0.15 \pm 0.27$	
Br (%)	2.03	2.0		1.63			
$\Lambda_b \to p l\nu$							
$\Gamma/\lvert V_{ub}\rvert^2$ (ps^{-1})	18.7	13.3	7.55			$25.7 \pm 2.6 \pm 4.6$	
Br (%)	0.045	0.029		0.0389	0.0254		
$\Lambda_b \to p \tau\nu$							
$\Gamma/\lvert V_{ub}\rvert^2$ (ps^{-1})	12.1	9.6	6.55			$17.7 \pm 1.3 \pm 1.6$	
Br (%)	0.029	0.021		0.0275			

Ratios of branching fractions

$$R_{\Lambda_c} = \frac{Br(\Lambda_b \to \Lambda_c \tau \nu)}{Br(\Lambda_b \to \Lambda_c l \nu)},$$
$$R_p = \frac{Br(\Lambda_b \to p \tau \nu)}{Br(\Lambda_b \to p l \nu)},$$
$$R_{\Lambda cp} = \frac{\int_{15\,\mathrm{GeV}^2}^{q^2_{max}} \frac{d\Gamma(\Lambda_b \to p\mu\nu)}{dq^2} dq^2}{\int_{7\,\mathrm{GeV}^2}^{q^2_{max}} \frac{d\Gamma(\Lambda_b \to \Lambda_c\mu\nu)}{dq^2} dq^2}.$$

Table 15: Predictions for the ratios of Λ_b baryon decay rates.

Ratio	our	Dutta	Lattice	Experiment (LHCb 2015)
R_{Λ_c}	0.313	0.3379	$0.3318 \pm 0.0074 \pm 0.0070$	
R_p	0.649	0.7071		
$R_{\Lambda cp}$	$(0.78 \pm 0.08)\frac{\lvert V_{ub}\rvert^2}{\lvert V_{cb}\rvert^2}$	0.0101	$(1.471 \pm 0.095 \pm 0.109)\frac{\lvert V_{ub}\rvert^2}{\lvert V_{cb}\rvert^2}$	$(1.00 \pm 0.04 \pm 0.08) \times 10^{-2}$

Comparing our result for $R_{\Lambda cp}$ with experimental data we find

$$\frac{|V_{ub}|}{|V_{cb}|} = 0.113 \pm 0.011|_{\rm theor} \pm 0.006|_{\rm exp},$$

in good agreement with the experimental ratio of these matrix elements extracted from inclusive decays

$$\frac{|V_{ub}|_{\rm incl}}{|V_{cb}|_{\rm incl}} = 0.105 \pm 0.006,$$

and with the corresponding ratio found in our previous analysis of exclusive semileptonic B and B_s meson decays [$|V_{cb}| = (3.90 \pm 0.15) \times 10^{-2}$, $|V_{ub}| = (4.05 \pm 0.20) \times 10^{-3}$]

$$\frac{|V_{ub}|}{|V_{cb}|} = 0.104 \pm 0.012.$$

Using lattice result one gets

$$\frac{|V_{ub}|}{|V_{cb}|} = 0.0083 \pm 0.004 \pm 0.004,$$

which for $|V_{cb}| = (3.95 \pm 0.08) \times 10^{-2}$ leads to

$$|V_{ub}| = (3.27 \pm 0.15 \pm 0.16 \pm 0.06) \times 10^{-3}$$

more than 3σ lower than $|V_{ub}|$ value extracted from inclusive decays

$$|V_{ub}|_{\rm incl} = (4.41 \pm 0.15^{+0.15}_{-0.19}) \times 10^{-3}$$

CONCLUSIONS

- Mass spectra of heavy and strange baryons were calculated in the relativistic quark model with the set of model parameters, fixed from previous considerations of meson properties.
- Light quarks, light diquarks and heavy quarks were treated fully relativistically without application of the nonrelativistic v/c and heavy quark $1/m_Q$ expansions.
- Baryons were considered in the framework of the relativistic quark–diquark picture.
- Internal structure of the diquark was taken into account by calculating the form factor of the diquark–gluon interaction.
- Masses of ground state, orbitally and radially excited heavy and strange baryons were calculated up to rather high excitations. This allowed to construct the Regge trajectories both in (J, M^2) and (n_r, M^2) planes. It was found that they are almost linear, parallel and equidistant.
- The assignment of the experimentally observed heavy and strange baryons to the particular Regge trajectories was carried out. This allowed to ascribe the quantum numbers to the excited heavy baryons.
- It was found that all currently available experimental data on heavy and strange baryons can be well described in the relativistic quark-diquark picture, which predicts significantly less states than the genuine three-body picture.
- Diquark and baryon wave functions obtained in calculating heavy baryon masses were used for the calculation of semileptonic decays.
- Structure of weak decay matrix elements agrees with model independent predictions of HQET both at leading and subleading orders of heavy quark expansion.
- Leading and subleading Isgur-Wise functions for heavy baryon decays were explicitly expressed through the overlap integrals of wave functions in the whole accessible kinematic range.
- Calculated decay rates agree with available experimental data.

BACKUP SLIDES

Table 16: Masses of the Σ_Q ($Q = c, b$) heavy baryons (in MeV).

$I(J^P)$	Qd state	$Q=c$ M	status	$M^{\exp}$	$Q=b$ M	status	$M^{\exp}$
$1(\frac{1}{2}^+)$	$1S$	2443	****	2453.76(18)	5808	***	5807.8(2.7)
$1(\frac{1}{2}^+)$	$2S$	2901			6213		
	$3S$	3271			6575		
	$4S$	3581			6869		
	$5S$	3861			7124		
$1(\frac{3}{2}^+)$	$1S$	2519	***	2518.0(5)	5834	***	5829.0(3.4)
	$2S$	2936	***	$2939.3(^{1.4}_{1.5})$?	6226		
	$3S$	3293			6583		
	$4S$	3598			6876		
	$5S$	3873			7129		
$1(\frac{1}{2}^-)$	$1P$	2799	***	$2802(^{4}_{7})$	6101		
	$2P$	3172			6440		
	$3P$	3488			6756		
	$4P$	3770			7024		
	$1P$	2713			6095		
	$2P$	3125			6430		
	$3P$	3455			6742		
	$4P$	3743			7008		
$1(\frac{3}{2}^-)$	$1P$	2798	***	$2802(^{4}_{7})$	6096		
	$2P$	3172			6430		
	$3P$	3486			6742		
	$4P$	3768			7009		

Table 16: (continued)

$I(J^P)$	Qd state	$Q=c$ M	status	$M^{\rm exp}$	$Q=b$ M	status	$M^{\rm exp}$
$1(\frac{3}{2}^-)$	$1P$	2773	*	2766.6(2.4)?	6087		
	$2P$	3151			6423		
	$3P$	3469			6736		
	$4P$	3753			7003		
$1(\frac{5}{2}^-)$	$1P$	2789			6084		
	$2P$	3161			6421		
	$3P$	3475			6732		
	$4P$	3757			6999		
$1(\frac{1}{2}^+)$	$1D$	3041			6311		
	$2D$	3370			6636		
$1(\frac{3}{2}^+)$	$1D$	3043			6326		
	$2D$	3366			6647		
	$1D$	3040			6285		
	$2D$	3364			6612		
$1(\frac{5}{2}^+)$	$1D$	3038			6284		
	$2D$	3365			6612		
	$1D$	3023			6270		
	$2D$	3349			6598		
$1(\frac{7}{2}^+)$	$1D$	3013			6260		
	$2D$	3342			6590		

Table 17: Masses of the positive parity Ξ states (in MeV).

J^P	Experiment			Theory					
	State	Status	Mass	Our	Capstick Isgur	Loring et al.	Melde et al.	Santopinto Ferretti	Engel et al.
$\frac{1}{2}^+$	Ξ	****	1321.71(7)	1330	1305	1310	1348	1317	1303(13)
				1886	1840	1876	1805	1772	2178(48)
				1993	2040	2062		1868	2231(44)
				2012	2100	2131		1874	2408(45)
				2091	2130	2176			
				2142	2150	2215			
				2367	2230	2249			
$\frac{3}{2}^+$	$\Xi(1530)$	****	1531.80(32)	1518	1505	1539	1528	1552	1553(18)
				1966	2045	1988		1653	2228(44)
				2100	2065	2076			2398(52)
				2121	2115	2128			2574(52)
				2122	2165	2170			
				2144	2170	2175			
				2149	2210	2219			
				2421	2230	2257			
$\frac{5}{2}^+$				2108	2045	2013			
				2147	2165	2141			
				2213	2230	2197			
$\frac{7}{2}^+$				2189	2180	2169			

Table 18: Masses of the negative parity Ξ states (in MeV).

J^P	Experiment			Theory					
	State	Status	Mass	Our	Capstick Isgur	Loring et al.	Melde et al.	Santopinto Ferretti	Engel et al.
$\frac{1}{2}^-$				1682	1755	1770			1716(43)
				1758	1810	1922			1837(28)
				1839	1835	1938			1844(43)
				2160	2225	2241			2758(78)
				2210	2285	2266			
				2233	2300	2387			
				2261	2320	2411			
$\frac{3}{2}^-$				1764	1785	1780	1792	1861	1894(38)
	$\Xi(1820)$	***	1823(5)	1798	1880	1873		1971	1906(29)
				1904	1895	1924			2426(73)
				2245	2240	2246			2497(61)
				2252	2305	2284			
				2350	2330	2353			
				2352	2340	2384			
$\frac{5}{2}^-$				1853	1900	1955	1881		
				2333	2345	2292			
				2411	2350	2409			
$\frac{7}{2}^-$				2460	2355	2320			
				2474		2425			
$\frac{9}{2}^-$				2502		2505			

Doubly heavy baryons

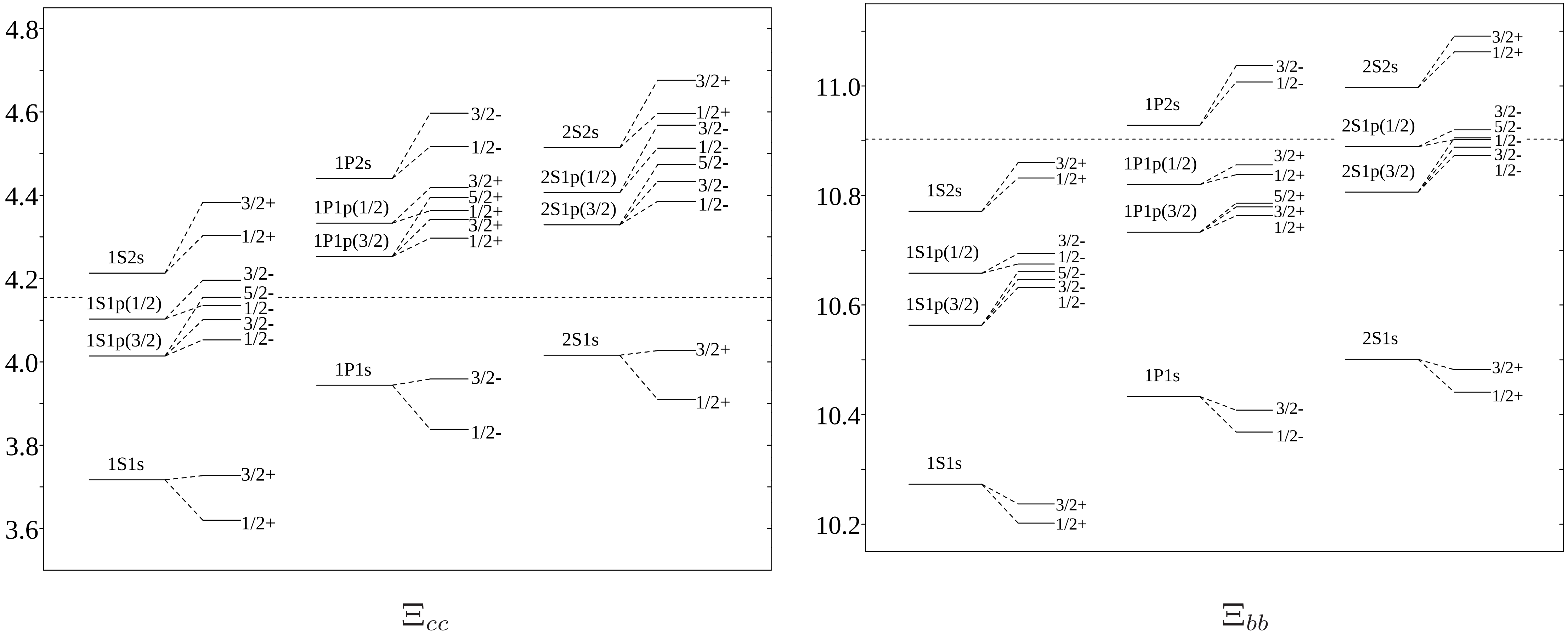

Figure 9: Mass spectrum of Ξ_{cc} and Ξ_{bb} baryons. The horizontal dashed line shows the $\Lambda_c D$ and $\Lambda_b D$ thresholds.

Table 19: Mass spectrum of ground states of doubly heavy baryons (in GeV). Comparison of different predictions. $\{QQ\}$ denotes the diquark in the axial vector state and $[QQ]$ denotes diquark in the scalar state.

Baryon	Quark content	J^P	our	Gershtein et al.	Ebert et al.	Roncaglia et al.	Körner et al.	Narodetskii Trusov
Ξ_{cc}	$\{cc\}q$	$1/2^+$	3.620	3.478	3.66	3.66	3.61	3.69
Ξ^*_{cc}	$\{cc\}q$	$3/2^+$	3.727	3.61	3.81	3.74	3.68	
Ω_{cc}	$\{cc\}s$	$1/2^+$	3.778	3.59	3.76	3.74	3.71	3.86
Ω^*_{cc}	$\{cc\}s$	$3/2^+$	3.872	3.69	3.89	3.82	3.76	
Ξ_{bb}	$\{bb\}q$	$1/2^+$	10.202	10.093	10.23	10.34		10.16
Ξ^*_{bb}	$\{bb\}q$	$3/2^+$	10.237	10.133	10.28	10.37		
Ω_{bb}	$\{bb\}s$	$1/2^+$	10.359	10.18	10.32	10.37		10.34
Ω^*_{bb}	$\{bb\}s$	$3/2^+$	10.389	10.20	10.36	10.40		
Ξ_{cb}	$\{cb\}q$	$1/2^+$	6.933	6.82	6.95	7.04		6.96
Ξ'_{cb}	$[cb]q$	$1/2^+$	6.963	6.85	7.00	6.99		
Ξ^*_{cb}	$\{cb\}q$	$3/2^+$	6.980	6.90	7.02	7.06		
Ω_{cb}	$\{cb\}s$	$1/2^+$	7.088	6.91	7.05	7.09		7.13
Ω'_{cb}	$[cb]s$	$1/2^+$	7.116	6.93	7.09	7.06		
Ω^*_{cb}	$\{cb\}s$	$3/2^+$	7.130	6.99	7.11	7.12		